2

Toward the microscopic understanding of conductance on a quantum mechanical basis

2.1 Quantum transport in metals

When Lew Dawydowitsch Landau[1] published his paper on the diamagnetism of metals [16], he was probably not aware of the importance of his calculation for quantum transport. In this publication he determined the quantized energy levels of free electrons in a homogeneous magnetic field

$$E_n = \hbar\omega_\mathrm{c}\left(n + \frac{1}{2}\right),$$

where $n \geq 0$ is an integer and $\omega_\mathrm{c} = eB/m$ is the cyclotron frequency. Similar calculations emphasizing the role of the sample edges were performed by V. Fock[2] [17], C.G. Darwin [18], and Edward Teller[3] [19]. The energy levels that we now call Landau levels played their first important role in experiments on the magnetoresistance of bismuth performed by L. Shubnikov and Wander Johannes de Haas[4] in 1930 [20]. They found that the measured magnetoresistance oscillated as a function of magnetic field, an effect now called *Shubnikov–de Haas effect*. A theoretical description of this effect was, for example, given in Ref. [21].

A full quantum mechanical description of electron transport was developed between 1950 and 1960 as a special case of quantum mechanical linear response theory. Kubo [22, 23] and Greenwood [24] were the first to propose a quantum theory of the conductance culminating in what is today known as the *Kubo–Greenwood formula* for the electrical conductance. It is based on linear response theory and takes at zero frequency and zero magnetic field the form [25]

[1] Lew Dawydowitsch Landau, ⋆ 22 January 1908, Baku, USSR, † 1 April 1968, Moscow, USSR; Nobel prize in physics 1962.

[2] Vladimir Alexandrovich Fock, ⋆ 22 December 1898, St Petersburg, Russia, † 27 December 1974, Leningrad, Russia.

[3] Edward Teller, ⋆ 15 January 1908, Budapest, Hungary

[4] Wander Johannes de Haas, ⋆ 2 March 1878, Lisse, Holland, † 26 April 1960, Bilthoven, Netherlands.

$$\boldsymbol{j}(\boldsymbol{x}) = \int \mathrm{d}^3x' \;\; \sigma(\boldsymbol{x},\boldsymbol{x}')\boldsymbol{\mathcal{E}}(\boldsymbol{x}'),$$

where

$$\sigma(\boldsymbol{x},\boldsymbol{x}') = h \int \mathrm{d}\alpha \;\int \mathrm{d}\beta \;\left[-\frac{\mathrm{d}f(E_\alpha)}{\mathrm{d}E}\right] \delta(E_{\beta\alpha})\boldsymbol{j}_{\beta\alpha}(\boldsymbol{x}) \otimes \boldsymbol{j}_{\alpha\beta}(\boldsymbol{x}'). \qquad (2.1)$$

Here the notion is that on the application of an electric field $\boldsymbol{\mathcal{E}}(\boldsymbol{x})$ the current created is described by the local current density $\boldsymbol{j}(\boldsymbol{x})$, which is a non-local microscopic reformulation of Ohm's law in eq. (1.1). The zero-frequency limit excludes time-dependent effects such as phonon scattering. We have introduced the non-local conductivity tensor $\sigma(\boldsymbol{x},\boldsymbol{x}')$, which can be calculated from the knowledge of the matrix elements of the current density $\boldsymbol{j}_{\alpha\beta}(\boldsymbol{x})$. The $\otimes$ symbol represents the tensor product of the two vectors. The basis states $|\,\alpha\,\rangle$ used for this representation are the exact eigenstates of the system's Hamiltonian including the disorder potential created by residual impurities and crystal imperfections at zero applied electric field. The quantities $E_{\alpha\beta} = E_\alpha - E_\beta$ are differences of eigenenergies. No impurity averaging has been performed in eq. (2.1). The temperature dependence of the conductivity enters through the Fermi–Dirac distribution function $f(E)$ [see eq. (1.5)]. Since in typical conduction problems the local electric $\boldsymbol{\mathcal{E}}(\boldsymbol{x})$ field is not known, it is frequently assumed to be homogeneous and the spatially averaged current density is calculated, resulting again in a local conductivity tensor.

It was shown, for example, by Kohn[5] and Luttinger [26] that such a quantum mechanical linear response theory for the conductance leads to the Drude–Boltzmann–Sommerfeld result in lowest order, if the electric field is homogeneous and *the average is taken over impurity configurations* in the system. The distribution function of the Boltzmann equation can be identified with the diagonal matrix elements of the density matrix in momentum representation. For macroscopic systems the familiar Boltzmann result for the energy-dependent elastic scattering rate [7, 27]

$$\frac{1}{\tau(E)} = N_\mathrm{i}\frac{m^\star}{(2\pi)^{d-1}\hbar^3}\left(\frac{2m^\star E}{\hbar^2}\right)^{d/2-1} \int \mathrm{d}\Omega_d \,|V(q)|^2\,(1-\cos\theta) \qquad (2.2)$$

is recovered, in which d is the dimension of the system, Ω_d is the solid angle in d dimensions, N_i denotes the volume density of the scatterers, $V(q)$ is the Fourier transform of the potential of an individual scatterer and $q = 2k\sin(\theta/2)$ and $k = \sqrt{2m^\star E/\hbar^2}$. The scattering time τ enters the expression for the conductivity in eq. (1.3). Equation (2.2) will be of particular importance in the analysis of our experimental results in part II of this book. Kohn and Luttinger recognized that beyond the semiclassical theory interference effects between scattered electron waves would lead to higher-order corrections. An important aspect of this approach to the description of transport is the fact that only properties of states at the Fermi-energy

[5] Walter Kohn, ⋆ 9 March 1923, Vienna, Austria, Nobel prize in chemistry 1998 (with J.A. Pople).

of the system enter the calculation of the conductance at zero temperature. The low-temperature conductance can therefore give some insight in the nature of the ground state of electronic systems.

At about the same time Rolf Landauer proposed a different theoretical view on the appearance of the resistance [28]. He considered the flow of electrons past an individual scattering center and predicted the presence of a resistivity dipole, today known as *Landauer's resistivity dipole*, around the scatterer. Such a resistivity dipole is essentially made up of electrons accumulating upstream and lacking downstream of the impurity, i.e., the electron gas is polarized around the impurity similar to a polarized atom in a dielectric material. For a one-dimensional conductor supporting a single mode, he found a formula for the conductance in the linear transport regime today known as the *Landauer formula* [29–32]

$$G = \frac{2e^2}{h}\frac{T}{1-T}, \tag{2.3}$$

in which T is the transmission probability for electrons through the conductor. This approach was later extended to the case of multimode and multiprobe conductors by M. Büttiker [33], leading to the Landauer–Büttiker formalism of the conductance. Its relation to the Kubo–Greenwood approach was clarified by Baranger and Stone in Ref. [34].

The quantum mechanical transmission is also of central importance for tunneling phenomena and Landauer's view on the resistance can also be applied to tunneling transport. Historically, already in 1928, i.e., soon after the formulation of quantum mechanics, Fowler and Nordheim investigated the field emission of electrons from metals [35]. The concept of inter-band tunneling in solids was proposed by Zener in 1943 [36] and in 1957, the Esaki diode[6] [37] made use of this concept. Tunneling through thin insulating layers from normal metals into superconductors [38] or between superconductors [39] studied around 1960 by I. Giaever[7] was the experimental technique used for verifying the existence of a superconducting energy gap and for measuring the density of states in superconductors. On the theoretical side, the transfer Hamiltonian approach was developed by John Bardeen[8] in Ref. [40]. The early work on tunneling in solids has been reviewed in Ref. [41].

[6] After Leo Esaki, ⋆ 12 March 1925, Osaka, Japan; Nobel prize in physics 1973 (with I. Giaever and B.D. Josephson)

[7] Ivar Giaever, ⋆ 5 April 1929, Bergen, Norway; Nobel price in physics 1973 (with L. Esaki and B.D. Josephson).

[8] John Bardeen, ⋆ 23 May 1908, Madison (Wisconsin), USA, † 30 January 1991, Boston, USA; Nobel prizes in physics 1956 (with W.H. Brattain and W. Shockley) and in 1972 (with L.N. Cooper and J.R. Schrieffer).

2.2 Transistors and two-dimensional electron gases in semiconductors

Parallel to the developments in fundamental research on conductance in the late 1950s, the remarkable technological success of microelectronics based on semiconducting materials began. In 1947/48 the transistor[9] was developed by John Bardeen, Walter Houser Brattain,[10] and William Shockley[11] at the Bell Laboratories on the basis of germanium. In 1954 the silicon technology started, the first transistor-based computer worked in 1955 in the United States and the concept of the integrated circuits was invented in 1958 by Jack St. Claire Kilby, engineer of Texas Instruments.

2.2.1 Two-dimensional electron gases in field-effect transistors

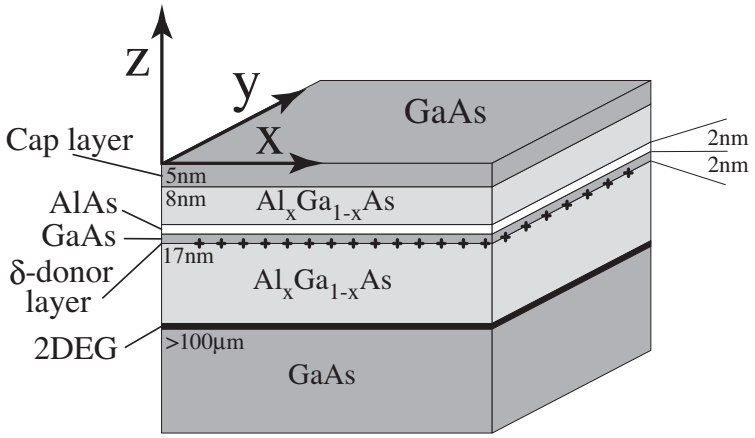

Fig. 2.1. Layer sequence in a GaAs/AlGaAs heterostructure. The two-dimensional electron gas (2DEG) forms at the interface between the two materials, here 34 nm below the sample surface.

From these early days on, fruitful mutual interactions began between the semiconductor industry and fundamental physics research. With the field-effect transistors,[12] two-dimensional electron gases became available for fundamental research

[9] From: **trans**fer res**istor**; the planar bipolar transistor was patented in 1948, mass production started in 1951; already in 1963 the worldwide production of transistors was 1 billion pieces, higher than the established electron tube.

[10] Walter Houser Brattain, ⋆ 10 February 1902, Amoy (today Xiamen, China), † 13 October 1987, Seattle, USA; Nobel prize in physics 1956 (with J. Bardeen and W. Shockley).

[11] William Shockley, ⋆ 13 February 1910, London, England, † 12 August 1989, Stanford (California), USA; Nobel prize in physics 1956 (with J. Bardeen and W.H. Brattain).

[12] the most famous variant is the silicon based MOSFET – **M**etal-**O**xide **F**ield **E**ffect **T**ransistor

in the 1960s and 1970s, initially based on the elemental semiconductors, silicon and germanium, later also on III-V compounds like gallium arsenide, aluminium arsenide, and others. These systems opened a new research area, namely, the physics of the electronic properties of two-dimensional systems (see Refs. [42, 43]). Figure 2.1 shows an example of a GaAs/AlGaAs heterostructure similar to the ones used in parts III and IV of this book for experiments. The two-dimensional electron gas (2DEG) accumulates at the interface between the two materials. Structures with very high crystal purity (typically less than 10^{14} cm^{-3} residual impurity concentration) can, for example, be grown by molecular beam epitaxy (MBE). Growth is based on GaAs (100) wafers on top of which a thick layer of GaAs is grown. Subsequently, the growth continues with an AlGaAs alloy that is almost perfectly lattice-matched to the GaAs cystal. Atomically sharp interfaces between these materials can be realized without introducing lattice distortions or interrupting the lattice periodicity. A lattice plane remote from the GaAs/AlGaAs interface is doped with silicon incorporated mainly on gallium lattice sites (n-type δ-doping). The layer sequence is completed by burying the doping plane in AlGaAs and capping the structure with a thin GaAs layer in order to prevent strong surface oxidation of the AlGaAs.

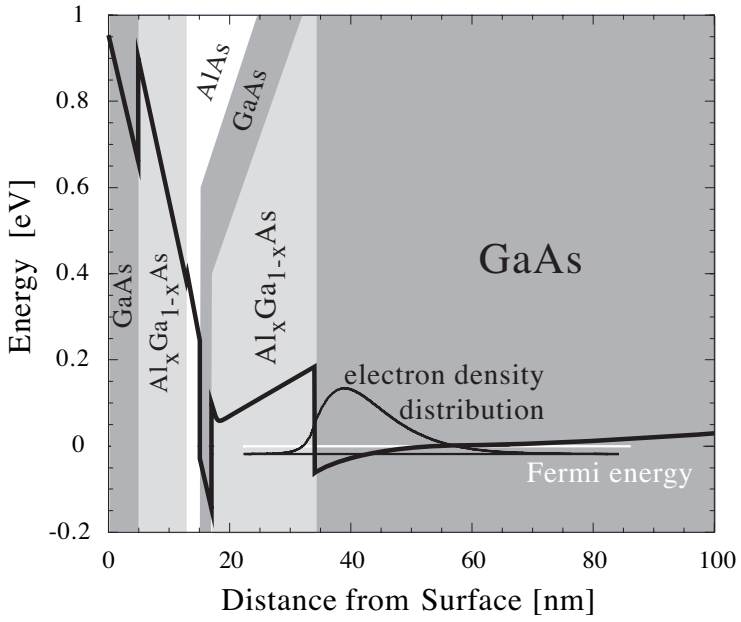

Fig. 2.2. Self-consistent conduction band profile of the GaAs/AlGaAs heterostructure

The resulting self-consistent conduction band structure of such a sample is shown in Fig. 2.2. The electrochemical potential of the system is pinned deep inside the GaAs substrate layer, typically close to the middle of the bandgap. At the interface

between GaAs and AlGaAs, a triangular potential well gives rise to a single occupied quantum state confining electrons to a thin sheet (about 10 nm thick). The thickness of the sheet in growth direction is given by the extent of the quantum state and can in principle not be made thinner due to arguments based on the uncertainty principle. The conduction band minimum rises strongly toward the surface, since at the surface the electrochemical potential is pinned by surface states in the bandgap of GaAs. The presence of this built-in barrier together with the insulating character of the AlGaAs barrier material allows the application of electric fields between the two-dimensional electron gas and a metallic gate electrode evaporated onto the surface of such a sample. The electron density can then be controlled via the field effect.

Electron transport in two-dimensional electron gases is routinely characterized and described in terms of the Drude–Boltzmann theory of transport in metals described above. Magnetotransport experiments in the spirit of Fig. 1.1 apply a current I to the two-dimensional system patterned into a Hall bar structure and the longitudinal and transverse voltages, U and U_{H}, respectively, are measured. If W is the width of the Hall bar and L is the separation between longitudinal voltage probes, the components of the two-dimensional resistivity tensor

$$\varrho = \begin{pmatrix} \varrho_{xx} & \varrho_{xy} \\ -\varrho_{xy} & \varrho_{xx} \end{pmatrix}$$

can be determined to be

$$\varrho_{xx} = \frac{W}{L}\frac{U}{I} \quad \text{and} \quad \varrho_{xy} = \frac{U_{\mathrm{H}}}{I}.$$

The corresponding conductivity tensor σ is obtained from ϱ by tensor inversion. The electron density (Hall density) n_{H} can then be determined from the low magnetic field Hall resistivity, which is linear in magnetic field B

$$n_{\mathrm{H}} = \frac{1}{e\,\mathrm{d}\varrho_{xy}(B)/\mathrm{d}B|_{B=0}}$$

and the Hall mobility $\mu_{\mathrm{H}} = e\tau/m^\star$ of the electrons follows from

$$\mu_{\mathrm{H}} = \frac{\mathrm{d}\varrho_{xy}(B)/\mathrm{d}B|_{B=0}}{\varrho_{xx}(0)}.$$

Typical values for electron densities in such two-dimensional systems at liquid helium temperatures range from $10^{14}\,\mathrm{m}^{-2}$ to $10^{16}\,\mathrm{m}^{-2}$, mobilities are typically between $0.1\,\mathrm{m}^2/(\mathrm{Vs})$ to $1000\,\mathrm{m}^2/(\mathrm{Vs})$. From the mobility μ_{H} one finds the scattering time τ, if the effective mass of the charge carriers is known. For electrons in GaAs, for example, the effective mass $m^\star = 0.067$ and a mobility of $100\,\mathrm{m}^2/(\mathrm{Vs})$ corresponds to a scattering time $\tau = 38\,\mathrm{ps}$. The Hall density allows the determination of the Fermi wave vector of the electrons via

$$k_{\mathrm{F}} = \sqrt{2\pi n_{\mathrm{H}}}$$

and the related Fermi wavelength λ_F, Fermi velocity v_F, and Fermi energy E_F. For an electron density of $5 \times 10^{15}\,\mathrm{m}^{-2}$ in GaAs, one obtains $\lambda_\mathrm{F} = 2\pi/k_\mathrm{F} = 35\,\mathrm{nm}$, $v_\mathrm{F} = \hbar k_\mathrm{F}/m^\star = 3 \times 10^5\,\mathrm{m/s}$, and $E_\mathrm{F} = \hbar^2 k_\mathrm{F}^2/(2m^\star) = 17.9\,\mathrm{meV}$. Combining information about the electron density and the mobility, the elastic mean free path can be determined from

$$l_\mathrm{e} = v_\mathrm{F}\tau$$

and the diffusion constant is given by

$$D = \frac{1}{2}v_\mathrm{F}^2\tau = \frac{1}{2}v_\mathrm{F}l_\mathrm{e}.$$

In a high-quality two-dimensional electron gas in GaAs with $n_\mathrm{H} = 5 \times 10^{15}\,\mathrm{m}^{-2}$ and a mobility $\mu_\mathrm{H} = 100\,\mathrm{m}^2/(\mathrm{Vs})$, one has $D = 1.8\,\mathrm{m}^2/\mathrm{s}$ and $l_\mathrm{e} = 11.7\,\mu\mathrm{m}$, which is already a macroscopic length scale. Similar electron gases form the basis for the measurements discussed in parts III and IV of this book.

The Shubnikov–de Haas effect in two-dimensional systems is another common measurement allowing the determination of the carrier density. The observed quantum oscillations in the resistance are periodic in $1/B$ [42]. The period $\Delta(1/B)$ is related to the Shubnikov–de Haas density via

$$n_\mathrm{SdH} = \frac{2e}{h\Delta(1/B)},$$

if spin-degenerate Landau levels are assumed. If the two-dimensional electron or hole gas is in the quantum limit (only one subband is occupied), then the Shubnikov–de Haas density and the Hall density are typically measured to be the same within a few percent. A more detailed analysis of the Shubnikov–de Haas effect allows the extraction of a quantum life-time of an electron in a Landau level and of the effective mass $m^\star$ [44, 45].

2.2.2 Resonant tunneling in semiconductors

In addition to the field-effect transistors, the advances in semiconductor material quality made the development of double-barrier resonant tunneling structures possible. In these structures, a quantum well extended in two dimensions is coupled via tunneling barriers to emitter and collector electrodes. The weak coupling leads to well separated quantized energy levels in the quantum well. If on the application of an external bias voltage occupied emitter states become resonant with quantum well states, resonant tunneling transport can occur through the structure. A further increase in the bias voltage detunes the resonant levels and as a consequence a negative differential resistance arises. This was first demonstrated by Leo Esaki and coworkers in the early 1970s [46, 47]. The resonant tunneling effect has to be mentioned here, because it is at the heart of tunneling transport through semiconductor quantum dot structures, which will be discussed in part III of this book.

2.2.3 Integer and fractional quantum Hall effect

In the early 1980s research on magnetotransport in two-dimensional electron gases was greatly stimulated by the experimental observation of important quantum phenomena: the integer quantum Hall effect found in silicon MOSFETs by Klaus von Klitzing[13] in 1980 [48] impressively showed the precise quantization of the Hall resistance U_{H}/I in integer fractions of the resistance quantum h/e^2 [c.f. eqs. (1.2) and (1.4)]:

$$\frac{U_{\mathrm{H}}}{I} = \frac{h}{e^2}\frac{1}{\nu},$$

where $\nu > 0$ is an integer called the "filling factor" of Landau levels. Figure 2.3

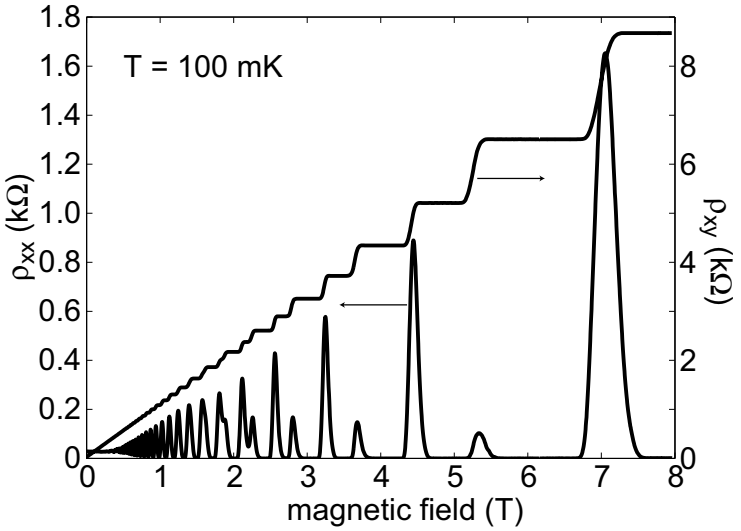

Fig. 2.3. Quantum Hall effect measured in a GaAs/AlGaAs heterostructure at a temperature of 100 mK. At magnetic fields where the Hall resistivity $\varrho_{xy} = U_{\mathrm{H}}/I$ shows plateaus, the longitudinal resistivity ϱ_{xx} is exceedingly small.

shows the quantum Hall effect measured on a high-quality GaAs/AlGaAs heterostructure at a temperature of 100 mK. The quantization of the Hall resistance at integer fractions of h/e^2 can be seen in the Hall resistivity ϱ_{xy}. At magnetic fields where the Hall resistivity shows plateaus, the longitudinal resistivity of the sample, ϱ_{xx}, is close to zero. Büttiker suggested a phenomenological and transparent description of the integer quantum Hall effect in terms of the transmission of edge channels [49]. The self-consistent nature of edge channels predicted by Chklovskii and coworkers in Ref. [50] will be further discussed in the scanning gate experiments described in chapter 16.

[13] Klaus von Klitzing, ⋆ 28 June 1943, Schroda, Poland; Nobel prize in physics 1985.

The fractional quantum Hall effect, where plateaus in ϱ_{xy} develop at fractional values of the filling factor ν, was discovered in gallium arsenide heterostructures by Tsui[14] and Störmer[15] [51] is based on the Coulomb interaction between electrons in two-dimensional systems leading to novel ground states. For example, an excellent approximate wave function for the $\nu = 1/3$ correlated many-body ground state was suggested by R. Laughlin[16] [52]. The fractional quantum Hall effect can be described as the integer quantum Hall effect of novel quasiparticles called composite fermions (see e.g. Refs. [53–56] for an introduction to the fractional quantum Hall effect).

2.2.4 Weak localization

In the late 1970s, two-dimensional electron gases were predicted to become insulating at zero magnetic field as the temperature approaches absolute zero. The predictions were based on the quantum interference of electrons leading to localization no matter how small the disorder potential due to residual crystal imperfections, an effect known as "weak localization" [57]. It turns out that the effect is closely related to the interference of elastically back-scattered electron waves. As a result of this finding, experimentalists working on two-dimensional systems were able to study phase-coherence phenomena — a still insufficiently understood topic reaching into fundamental quantum mechanics. The weak localization effect has a logarithmic temperature dependence, and it can be suppressed by applying a magnetic field normal to the plane of the two-dimensional system. This is shown in Fig. 2.4 for a p-SiGe sample measured at a temperature of 100 mK. The weak localization effect

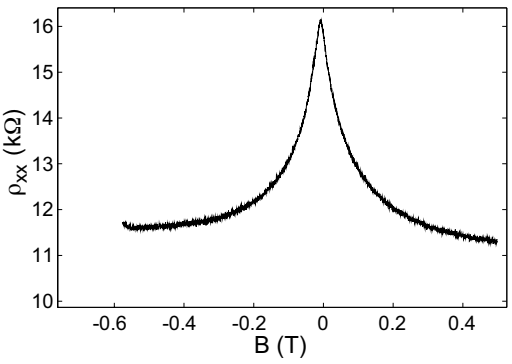

Fig. 2.4. Measurement of the suppression of the weak localization effect in a magnetic field. The sample is a p-SiGe quantum well with a two-dimensional hole gas.

will be discussed in much more detail in part II of this book where it plays a very

[14] Daniel C. Tsui, ⋆ 1939, Henan, China; Nobel prize in physics 1998 (with H.L. Störmer and R.B. Laughlin).

[15] Horst L. Störmer, ⋆ 6 April 1949, Frankfurt am Main, Germany; Nobel prize in physics 1998 (with R.B. Laughlin and D.C. Tsui).

[16] Robert Laughlin, ⋆ 1 November 1950, Visalia, California, USA; Nobel prize in physics 1998 (with H. Störmer and D.C. Tsui).

important role in connection with a possible metal–insulator transition in strongly interacting two-dimensional systems at zero magnetic field.

2.3 Basic phenomena in semiconductor structures of reduced size and dimensionality

2.3.1 The Aharonov–Bohm effect and conductance fluctuations

Already in 1939 it was pointed out by Franz [58] that two electron beams enclosing a magnetic flux Φ between them would acquire a relative phase given by

$$\Delta\varphi = 2\pi\frac{\Phi}{\Phi_0},$$

where $\Phi_0 = h/e$ is the flux quantum. Later, Aharonov and Bohm[17] realized, that in contrast to the classical motion of a charged particle in an electromagnetic field where only the fields play a role, in the quantum description the electromagnetic potentials cannot be eliminated from the equations of motion [59]. They suggested interference experiments between electron waves that could prove the physical significance of the electromagnetic potentials. One of these experiments is schematically depicted in Fig. 2.5. This fundamental effect, nowadays called Aharonov–Bohm ef-

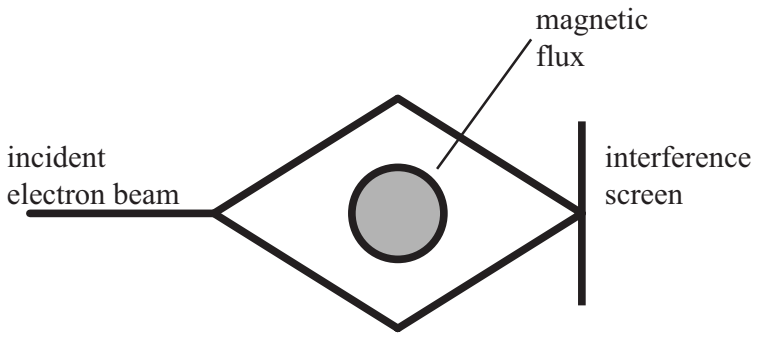

Fig. 2.5. Scheme of the interference experiment suggested by Aharonov and Bohm

fect, is not only the basis for the microscopic understanding of the weak localization phenomenon, but it became of great importance in the field of semiconductor structures with reduced dimensionality, which developed rapidly in the 1980s, certainly also inspired by the industrial requirements of smaller and faster electronic devices. In 1985 first indications of the Aharonov–Bohm effect were observed in

[17] David Joseph Bohm, ⋆ 26 December 1917, Wilkes-Barre, Pennsylvania, USA, † 27 October 1992.

double-quantum well structures [60] and later also in laterally defined semiconducting ring-shaped systems [61–64], at a time when this phenomenon was already well studied in metallic systems [65, 66]. A good introduction to the phenomenon is given in Ref. [67]. Figure 2.6a shows the Aharonov–Bohm effect measured in a ring structure of $d = 1\,\mu\text{m}$ diameter, realized on a GaAs/AlGaAs heterostructure. Periodic oscillations of the resistance as a function of magnetic field are clearly visible. The period of about 4 mT corresponds to the magnetic flux $\Phi = B\pi d^2/4$ through the ring being an integer number times the flux quantum Φ_0. This Aharonov–Bohm period will play an important role in chapter 12, where we show measurements of the Coulomb-blockade effect (see below) in a ring geometry.

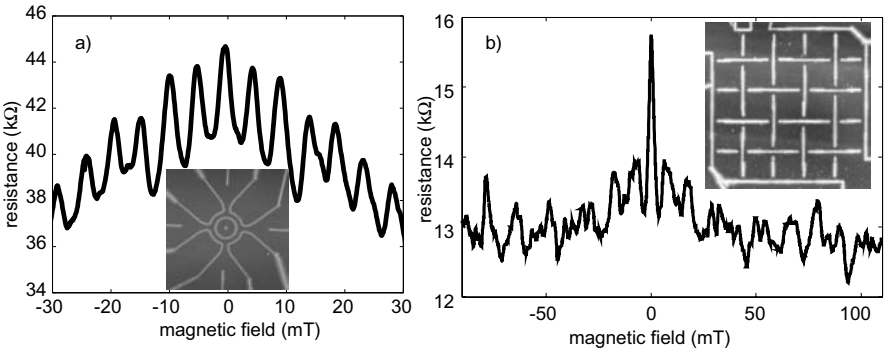

Fig. 2.6. a) Aharonov–Bohm effect measured at a temperature of 30 mK in the quantum ring structure shown in the inset. The current driven through the ring was 1.7 nA. The period of the oscillations of about 4 mT corresponds to the area of the ring with radius $r = 0.5\,\mu\text{m}$. b) Conductance fluctuations measured in a sample in which 1 µm square cavities are arranged in a 5×5 array (see inset). Neighboring cavities are coherently coupled via small openings. The characteristic field scale of the fluctuations is again 4 mT corresponding to $1\,\mu\text{m}^2$, the area of an individual cavity.

The search of the Aharonov–Bohm effect in metals and also in semiconductor structures was hindered by the presence of another related interference effect, namely, the conductance fluctuations, which manifest themselves as aperiodic but reproducible fluctuations in the resistance of a sample as a function of an external parameter such as the magnetic field or the electron density. Conductance fluctuations occur in samples whose characteristic size L is of the order of the phase coherence length l_φ of the electrons. They occur in systems where the elastic mean free path of the electrons l_e is much smaller than L (then called universal conductance fluctuations, or UCF), or in classically chaotic systems if $l_\text{e} \gg l_\varphi$ (then called ballistic conductance fluctuations). A substantial discussion of conductance fluctuations can be found in Refs. [30, 32]. An example of ballistic conductance fluctuations is depicted in Fig. 2.6b [68]. They were measured at 100 mK on a sample in which an array of 5×5 ballistic cavities of size $1 \times 1\,\mu\text{m}^2$ was realized. Neighboring cavities were

interconnected by narrow constrictions. The sample was based on a GaAs/AlGaAs heterostructure.

In general, structures in which the electronic phase coherence length l_φ is comparable to the characteristic system size L but much larger than the Fermi wavelength λ_F are called *mesoscopic systems*. Depending on the relation between the mean free path of the electrons l_e and the system size L, one talks about ballistic ($l_\mathrm{e} \gg l_\varphi$) or diffusive ($l_\mathrm{e} \ll l_\varphi$) systems.

2.3.2 Conductance quantization in semiconductor quantum point contacts

In 1988 the quantization of the conductance in very narrow constrictions in a two-dimensional electron gas was discovered by van Wees and coworkers [69] and Wharam and coworkers [70]. They were able to vary the width of the constriction from less than one to many Fermi wavelengths by applying voltages to a split-gate. They found that with increasing gate voltage, i.e., increasing width of the constriction, the conductance did not increase linearly, as expected from purely classical arguments, but it increased in steps of $2e^2/h$. An example of this effect is shown in Fig. 2.7. It turns out that the effect can most naturally be described by the Landauer–Büttiker formula

$$G = \frac{2e^2}{h} NT, \tag{2.4}$$

where N is the number of transverse modes in the constriction with average transmission $T = 1$. This formula differs from eq. (2.3) in the appearance of the factor N and in the fact that only the transmission T appears instead of $T/(1-T)$. In fact, the latter goes to infinity as T approaches 1. The reason for a finite conductance despite the absence of scattering is the fact that the electron gas has to couple adiabatically from a very large (infinitely large) reservoir into a narrow constriction, which gives rise to the "contact" resistance $R_\mathrm{c} = h/(2e^2N)$. If this resistance is coupled in series with the pure resistance of the constriction in analogy to eq. (2.3), $R_\mathrm{s} = [h/(2e^2N)](1-T)/T$, then we indeed recover eq. (2.4) [31]. Further details about the conductance quantization can be found in Refs. [30–32]. A very clear

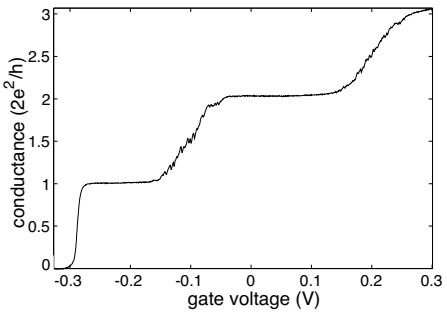

Fig. 2.7. Conductance quantization in a quantum point contact realized on a GaAs/AlGaAs-heterostructure. The plateaus in the conductance are reminiscent of the plateaus in the quantum Hall effect in Fig. 2.3.

discussion of the effect in terms of the adiabatic approximation was given in Refs. [32, 71]. Although quantum point contacts are interesting research objects themselves (see e.g. Ref. [72] for an interesting recent publication), they also form the basic element for the fabrication of more complex nanostructures such as quantum dots (see below in this chapter and part III).

If constrictions are made long and thin, the resulting structures are called quantum wires. These systems are interesting because they are tunable one-dimensional systems. In the terminology of mesoscopic physics, a system becomes one dimensional as soon as its width W becomes smaller than the phase-coherence length l_φ. Such wires will be investigated with scanning gate techniques in chapter 17. A strictly one-dimensional system in the quantum mechanical sense, however, is reached only if W is comparable to $\lambda_\mathrm{F}/2$, which means that only one mode is occupied. Experimentally, such systems are difficult to realize. Even in wider mesoscopically one-dimensional systems, the quantization of the conductance is lost because imperfections in the wires do not allow T to approach unity. The resulting backscattering in such wires leads to the observation of conductance fluctuations. Exceptions are very pure quantum wire fabricated by cleaved-edge overgrowth, which indeed show conductance quantization in spite of their length [73].

2.3.3 Semiconductor quantum dots and artificial atoms

At about the same time as the discovery of conductance quantization, another important effect was found in mesoscopic semiconductor structures and in mesoscopic metallic devices. If a small conducting island of charge is coupled to two large electron reservoirs (source and drain contacts) via quantum point contacts driven into pinch-off, the conductance of the device becomes much smaller than the conductance quantum $2e^2/h$. The current–voltage characteristics of such devices are highly nonlinear at very low temperatures (about 100 mK) showing an exponential suppression of the current at low bias. When a gate electrode is placed next to the island, the conductance as a function of gate voltage exhibits a series of thermally broadened peaks with extremely small conductance in between. Such a measurement made on a quantum dot realized on a GaAs heterostructure is shown in Fig. 2.8. The suppression of the conductance in the valleys between peaks is called the Coulomb-blockade effect. Its origin is the classical Coulomb repulsion of electrons. It leads to a charging energy of the almost isolated island characterized by the energy scale

$$\Delta E_\mathrm{c} = \frac{e^2}{2C}.$$

Here, C is the capacitance of the island. The separation of neighboring conductance peaks is closely related to the charging energy. While in the Coulomb-blockade regions the number of electrons on the island is constant, on a conductance peak it can change by one thus allowing a current to flow. On a conductance peak, a single electron enters and leaves the island before the next electron can enter. In this sense, such islands are called *single-electron transistors* (SETs). Although experiments on metallic grains embedded in thin insulating films were already investigated

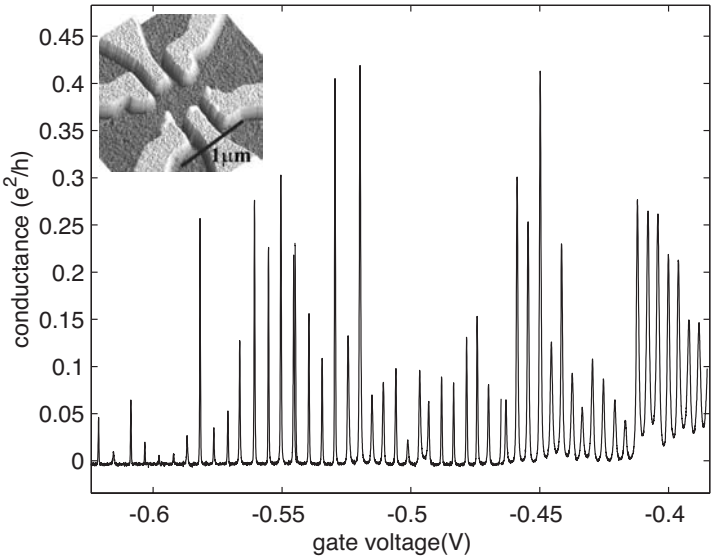

Fig. 2.8. Coulomb blockade in the conductance of a semiconductor quantum dot. The inset shows a scanning electron microscope image of the gate-defined quantum dot structure.

in the 1950s and 1960s [74–76] and a transport theory was developed by Kulik and Shekhter [77], the first indication for the Coulomb-blockade effect in an individual artificially fabricated metallic SET was reported by Fulton and Dolan in Ref. [78]. First results in semiconducting samples were obtained by Scott-Thomas and coworkers [79] looking at inhomogeneous wires in Si-MOSFET inversion channels. In the 1990s, semiconducting islands containing very few (down to one) electrons could be fabricated by Tarucha and coworkers [80, 81]. These quantum dots showed shell filling effects and are therefore referred to as *artificial atoms*. In 1997 the Kondo effect in an artificial quantum dot was found by Goldhaber-Gordon and coworkers [82]. This effect, which is well known from dilute magnetic alloys (see Ref. [83]) had been predicted to occur in quantum dots with an unpaired spin in the regime of relatively strong coupling to source and drain [84–86].

Electron transport through quantum dots is discussed in a number of books [32, 87–90] and review articles [81, 91–95]. An introduction to the subject is given in chapter 11 as a preparation for the subsequent description of measurements on quantum dots and quantum rings.

Part II

Conductance in Strongly Interacting and Disordered Two-Dimensional Systems

The physics of electron transport in two-dimensional systems has been intensely investigated in the 1970s and early 1980s. With the availability of Si-MOSFETs (Silicon Metal-Oxide-Field-Effect-Transistors) and GaAs/AlGaAs heterostructures, two-dimensional electron gases could be probed at low temperatures and in magnetic fields. The effects of disorder and interactions could be demonstrated convincingly. The theoretical description has been built on Fermi-liquid concepts and found to agree well with experiments.

With increasing sample quality (in both material systems, Si and GaAs) and the advent of other high-quality two-dimensional systems like p-GaAs heterostructures or n- and p-SiGe structures, a new range of parameters became accessible. Carrier densities could be driven to very low values, where interactions among electrons or holes become more and more important, without entering the strongly localized regime. In the mid-1990s experiments were performed that had an enormous impact on the community and lead to speculations about a metal–insulator transition in two-dimensional systems at zero magnetic field.

In the following chapters a perspective of this very active field of research is presented and results obtained on the p-SiGe system are discussed in detail. In chapter 3 to 7 we introduce the well-established theoretical concepts based on Fermi-liquid theory and beyond. In chapters 8 and 9 an overview is given of experiments and theories related to the possible metal–insulator transition in two-dimensions. Chapter 10 will be devoted to experiments performed on p-SiGe quantum wells which exhibit features of the metal–insulator transition, their analysis, and interpretation.

http://www.springer.com/978-0-387-40096-9

Electronic Quantum Transport in Mesoscopic Semiconductor Structures

Ihn, Th.

2004, 270 p. 81 illus., 7 illus. in color., Hardcover
ISBN: 978-0-387-40096-9